

ADDITION OF SILVER AND TITANIUM DIOXIDE NANOPARTICLES TO REAL-TIME PCR FOR THE DETECTION *ASPERGILLUS* SPP. AND AFLATOXIN GENES

M.A. MAHMOUD^{a*}, M.I. AFIFI^b, M.R. AL-OTHMAN^c, A.R.M. ABD EL-AZIZ^c

^a*Plant Pathology Research Institute, Agricultural Research Center, Giza, Egypt.*

^b*Biochemistry Department, Faculty of Agriculture, Ain Shams University, Cairo, Egypt.*

^c*Botany and Microbiology Department, College of Science, King Saud University, Riyadh 1145, Kingdom of Saudi Arabia.*

The unique properties of nanoparticles (NPs) and their interactions with biological systems, especially in biochemical reactions, provide many potential applications in molecular biology methods. Most of works have focused on gold NPs only, and many other kinds of NPs such as silver (Ag) and titanium dioxide (TiO₂) NPs have been largely neglected. Therefore, in this study, we evaluated the effect of Ag-NPs and TiO₂-NPs on the real-time PCR (RTi-PCR) detection of four *Aspergillus* spp., *A. flavus*, *A. parasiticus*, *A. ochraceus*, and *A. fumigatus*, and four aflatoxin biosynthesis genes (*tub1*, *aflR*, *aflD*, and *aflM*) in *A. flavus*. Several combinations of Ag-NPs and TiO₂-NPs at 3 μL and 5 μL were tested. The results showed that the Ag-NPs alone exhibited partial inhibition of RTi-PCR at 3 μL. Combinations of Ag-NPs and TiO₂-NPs (1:1, 2:1, 3:1) also partially inhibited RTi-PCR, but TiO₂-NPs alone and their combinations with Ag-NPs (2:1 and 3:1) caused complete RTi-PCR inhibition. All combinations of Ag-NPs and TiO₂-NPs at 5 μL resulted in complete inhibition of RTi-PCR, except for the 2:1 combination of Ag-NPs to TiO₂-NPs. The results indicate that effects on the assay detection system must be carefully evaluated before Ag-NPs and TiO₂-NPs are included in any RTi-PCR assay.

(Received August 18, 2017; Accepted October 21, 2017)

Keywords: Silver and titanium dioxide nanoparticles, real-time PCR, Detection *Aspergillus* spp., aflatoxin genes

1. Introduction

Nanotechnology, which is technology at the scale of one-billionth of a meter, is a rapidly growing field crossing boundaries among physics, chemistry, and biology [1]. Biotechnology is the combination of biology and technology that is developed to provide benefits and quality improvement in all fields related to human welfare [2]. Conventional polymerase chain reaction (PCR) and real-time (RTi)-PCR are integral components of biotechnology, and arguably represent the most powerful laboratory techniques ever developed. PCR is a technique that allows for the amplification of specific DNA segments in vitro [3] and is currently widely used in genetic identification, clinical microbiology, drug development, and in the agricultural, environmental, and forensic sciences [1,4]. Bionanotechnology is one of the most promising technologies of the 21st century, which integrates biotechnology and nanotechnology. This integration has provided an unprecedented opportunity to develop new tools for medical, industrial, agricultural, and environmental applications [5]. Many researchers working on the interactions between nanoparticles (NPs) and nucleic acids have begun to explore carbon [6], silica [7], gold (Au) [8], silver (Ag) [9], and iron/magnetic [10] NPs, thereby promoting their applications in molecular biology research. Bioconjugate-nano-PCR has been developed as a rapid and specific diagnosis

*Corresponding author: m.a.mahmoud75@gmail.com

method for the identification of *Candida* spp. AuNP- and AgNP-assisted PCR shows improved sensitivities and specificities compared to conventional PCR assays with very low PCR cycle numbers and amounts of concentrated DNA required [11]. Titanium oxide (TiO₂)-NPs showed significant enhancement over the traditional PCR efficiency for various types of templates (genomic DNA, plasmid DNA, and complementary DNA). In particular, the incorporation of TiO₂-NPs increased the amount of the PCR product by seven-fold and was less time consuming, with a 50% reduction in the time required for the denaturation and annealing steps [12]. However, [13] further evaluated the effects of Ag-NPs and TiO₂-NPs in RTi-PCR, and found that the NPs caused partial or complete PCR inhibition, with a stronger inhibitory effect observed for TiO₂-NPs.

Moreover, [8] used Au-NPs to optimize classic PCR and RTi-PCR assays by amplifying DNA sequences from genetically modified canola. However, they could not provide conclusive evidence on the effect of Au-NPs on the PCR performance and melt curve contrast reported in previous studies, although the reactions appeared to show very good efficiency and high specificity in the absence of Au-NPs. This study indicated that inclusion of Au-NPs in classic PCR and RTi-PCR assays should be undertaken with caution, based on evaluations and validation of the use of Au-NPs under specific conditions for any PCR technique.

To further explore the potential and use of NPs in RTi-PCR, the aim of the present study was to evaluate the effect of Ag-NPs and TiO₂-NPs on RTi-PCR for the detection of four *Aspergillus* spp., *A. flavus*, *A. parasiticus*, *A. ochraceus*, *A. fumigatus*, and four aflatoxin biosynthesis genes (*tub1*, *aflR*, *aflD*, and *aflM*) in *A. flavus*.

2. Materials and Methods

2.1 Isolation, cultivation, and identification of *Aspergillus terreus* strain SDP9.

The fungus was isolated from the soil of date palm in Riyadh, Saudi Arabia, and incubated on potato dextrose agar at 28°C. Fungal isolates were molecularly identified on the basis of their internal transcribed spacer regions (ITS1-5.8S-ITS2) [14]. The isolate was registered in GenBank as *Aspergillus terreus* SDP9 (Accession Number: KC462061), which was also used for the biosynthesis of Ag-NPs and TiO₂-NPs.

2.2 Biomass preparation of *A. terreus* KC462061 and biosynthesis of Ag-NPs and TiO₂-NPs

To prepare biomass for the biosynthesis of Ag-NPs and TiO₂-NPs, *A. terreus* KC462061 was grown in liquid medium according to previously described methods [14].

Ag-NPs were synthesized using 50 mL of a 1 mM AgNO₃ solution following the method described by [14]. The solution was left to calcify at 180°C for 5 h for crystallization of the Ag-NPs. TiO₂-NPs were synthesized using a 50-mL aqueous solution of 0.025 M TiO₂ (pH 3.5) that was added to the mycelia mass (20 g wet weight) in a 250-mL Erlenmeyer flask, following the method described by [16].

2.3 Extraction of DNA for *Aspergillus* spp.

DNA was extracted from isolates of *A. flavus*, *A. parasiticus*, *A. ochraceus*, and *A. fumigatus* (Table 1) following the method described by [16]. This same method was used to extract DNA of the aflatoxin biosynthesis genes from the *A. flavus* isolate.

Table 1. Isolates of *Aspergillus* spp. used in this study.

No.	Origin	Source	Species name
1	Saudi Arabia	Wheat	<i>A. flavus</i>
2	Saudi Arabia	Corn	<i>A. parasiticus</i>
3	Saudi Arabia	Rice	<i>A. ochraceus</i>
4	Saudi Arabia	Wheat	<i>A. fumigatus</i>

2.4 RTi-PCR assays.

RTi-PCR amplifications were performed with a thermal cycler (LightCycler 2.0; Roche Diagnostics GmbH, Germany) using specific primers for *Aspergillus* spp. detection (Table 2) and detection of the aflatoxin biosynthesis genes of *A. flavus* (Table 3), as described in the references given in the respective tables. In each run, we added different concentrations of Ag-NPs and/or TiO₂-NPs (Table 4) at amounts of 3 μL and 5 μL.

Table 2. Sequences of primers and T_m for detection *Aspergillus* spp. by Rti-PCR assays

<i>Aspergillus</i> spp	Sequence	Melting temp. (°C)	Reference
<i>A. flavus</i>	FL1-F (5'-ATTCATGGCCGCCGGGGGCTCTCA-3')	87	[17]
	FL1-R (5'-GATTGATTTGCGTTCGGCAAGC-3')		
<i>A. fumigatus</i>	ITS (5'-TATGCAGTCTGAGTTGATTATCG-3')	92.7	[18]
	ITS (5'-ACCTTAGAAAAATAAAGTTGGGTG-3')		
<i>A. parasiticus</i>	FLAVIQ1 (5'-GTCGTCCCCTCTCCGG-3')	89.3	[19]
	PARQ2 (5'-GAAAAAATGGTTGTTTTGCG-3')		
<i>A. ochraceus</i>	OCAV(5'-ATACCACCGGCTAATGCA-3')	83	[20]
	OCAR (5'-TGCCGACAGACCGAGTGGATT-3')		

Table 3. Sequences of primers and T_m for aflatoxin biosynthesis genes by Rti-PCR assays

Gene	Sequence	Melting temp. (°C)	Reference
<i>tub1</i>	(5'-GTCCGGTGCTGGTAACAAC-3')	65	[21]
	(5'-GGAGGTGGAGTTTCCAATGA-3')		
<i>aflR</i>	(5'-CGCGCTCCAGTCCCCTTCATT -3')		
	(5'-CTTGTTCGCCGAGATGACCA-3')		
<i>aflD</i>	(5'-ACCGCTACG CCG GCACTCTCGGCAC-3')		
	(5'-GTTGGCCGCCAGCTTCGACACTCCG-3')		
<i>aflM</i>	(5'- GCCGCACGCGGAGAAAAGTGGT-3')		
	(5'- GGGGATATACTCCCGCGACACAGCC-3')		

Table 4. Concentration of Ag-NPs and TiO₂-NPs and different combinations of Ag-NPs and TiO₂-NPs with 3 μl and 5 μl

Code	Specification
m	Non Ag-NPs and TiO ₂ -NPs
m1	only Ag-NPs (100 μg/mL)
	combinations of AgNPs and TiO ₂ NPs
m2	2:1 (50 μg/mL and 25 μg/mL)
m3	3:1 (75 μg/mL and 25 μg/mL)
m4	1:1 (50 μg/mL and 50 μg/mL)
m5	only TiO ₂ -NPs (100 μg/mL)
m6	1:2 (25 μg/mL and 50 μg/mL)
m7	1:3 (25 μg/mL and 75 μg/mL)

3. Results and discussion

Fig. 1 showed morphology and shape of Ag-NPs and TiO₂-NPs by TEM. The present experiments were performed to evaluate the individual and combined effects of Ag-NPs and TiO₂-NPs on the RTi-PCR efficiency, using different concentrations of the NPs.

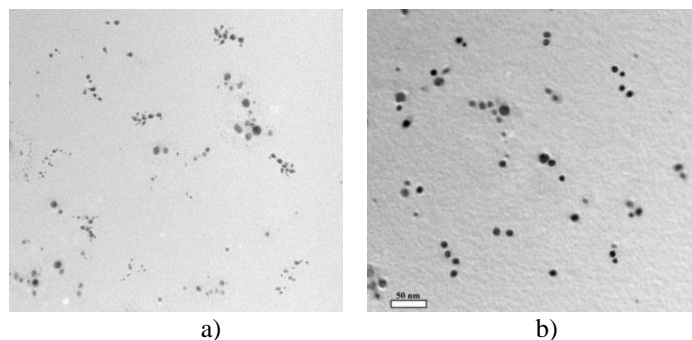


Fig. 1. TEM images of TiO_2 -NPs (a) and Ag-NPs (b)

The first experiment was conducted to detect four *Aspergillus* spp. (Fig. 2) using 3 μL mixtures of NPs in different concentrations or combinations. The results for the detection of *A. flavus* with and without NPs are shown in Figure 2a. The first curve appeared for mixture m (reference sample without NPs), and then curves for the mixtures m1, m2, m3, and m4, corresponding to Ag-NPs at concentrations of 25–100 $\mu\text{g}/\text{mL}$, appeared subsequently, indicating partial RTi-PCR inhibition. However, the mixtures m5, m6, and m7, corresponding to 25–100 $\mu\text{g}/\text{mL}$ TiO_2 -NPs, showed complete RTi-PCR inhibition. The amplification curves for the RTi-PCR detection of *A. parasiticus*, *A. ochraceus*, and *A. fumigatus* are shown in Figure 2 b, c, and d, respectively. Similar to the results for *A. flavus*, in all cases, the first curve appeared for mixture m (reference, no NPs). Mixtures m1–m4 showed partial RTi-PCR inhibition, whereas mixtures m5–m7 showed complete RTi-PCR inhibition.

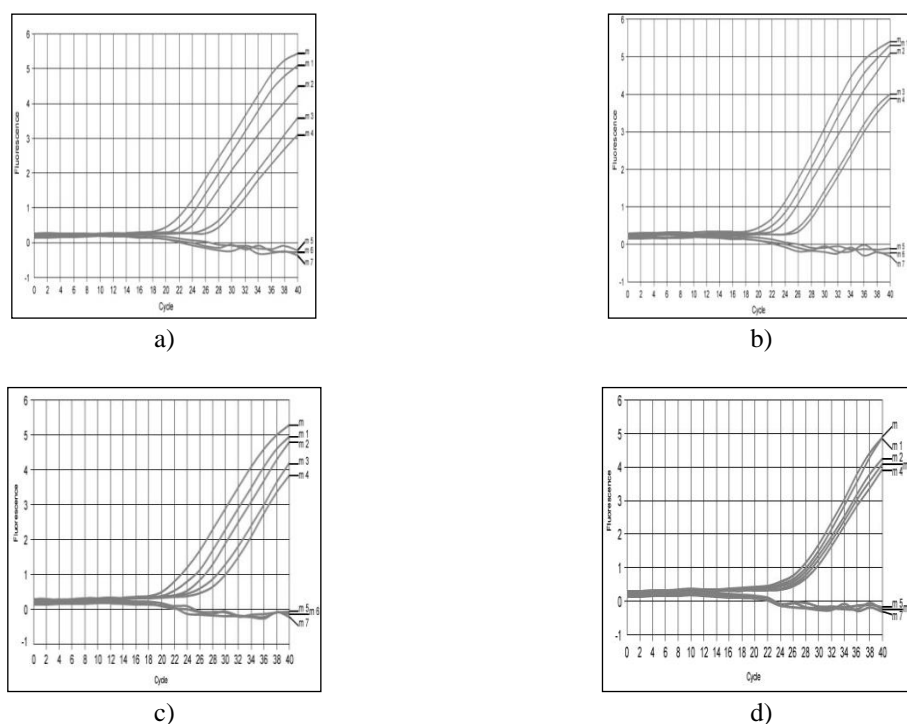


Fig. 2. Amplification curves of RTi-PCR for detection of a) *A. flavus*, b) *A. parasiticus* c) *A. ochraceus* d) *A. fumigatus* with 3 μL of different combinations of Ag-NPs and TiO_2 -NPs. (m) reference curve with no NPs, m1 with Ag-NPs at 100 $\mu\text{g}/\text{mL}$, m2 with Ag-NPs at 50 $\mu\text{g}/\text{mL}$ and TiO_2 -NPs at 25 $\mu\text{g}/\text{mL}$, m3 with Ag-NPs at 75 $\mu\text{g}/\text{mL}$ and TiO_2 -NPs at 25 $\mu\text{g}/\text{mL}$, m4, with Ag-NPs at 50 $\mu\text{g}/\text{mL}$ and TiO_2 -NPs at 50 $\mu\text{g}/\text{mL}$, m5 with TiO_2 -NPs at 100 $\mu\text{g}/\text{mL}$, m6 with TiO_2 -NPs at 50 $\mu\text{g}/\text{mL}$ and Ag-NPs at 25 $\mu\text{g}/\text{mL}$, m7 with TiO_2 -NPs at 75 $\mu\text{g}/\text{mL}$ and Ag-NPs at 25 $\mu\text{g}/\text{mL}$.

The second experiment was conducted to evaluate the effect of the 3- μL mixtures of the NPs on the detection of four aflatoxin biosynthesis genes (*tub1*, *aflR*, *aflD*, and *aflM*) of *A. flavus* Fig. 3. Fig. 3a shows the amplification curves for *tub1*, revealing that the four reactions (m1–m4) with pure Ag-NPs and three combinations of Ag-NPs and TiO₂-NPs (2:1, 3:1 and 1:1) exhibited partial RTi-PCR inhibition. Pure TiO₂-NPs and two combinations of TiO₂-NPs and Ag-NPs (1:1, 1:2, and 1:3) indicated to complete RTi-PCR inhibition was observed for the mixtures m5–m7. The same results were obtained for the detection of the *aflR*, *aflD*, and *aflM* genes, as shown in Fig. 3b, c, and d, respectively.

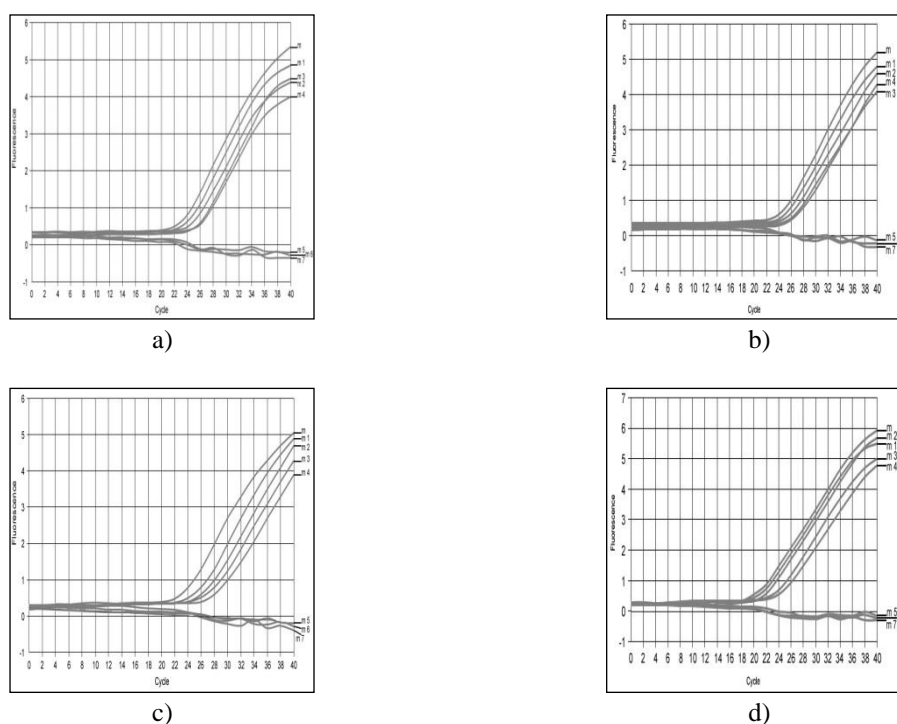


Fig. 3. Amplification curves of the four genes, a) *tub1*, b) *aflR*, c) *aflD* and d) *aflM* with 5 μL of different combinations of Ag-NPs and TiO₂-NPs. (m) reference curve with no NPs, m1 with Ag-NPs at 100 $\mu\text{g}/\text{mL}$, m2 with Ag-NPs at 50 $\mu\text{g}/\text{mL}$ and TiO₂-NPs at 25 $\mu\text{g}/\text{mL}$, m3 with Ag-NPs at 75 $\mu\text{g}/\text{mL}$ and TiO₂-NPs at 25 $\mu\text{g}/\text{mL}$, m4, with Ag-NPs at 50 $\mu\text{g}/\text{mL}$ and TiO₂-NPs at 50 $\mu\text{g}/\text{mL}$, m5 with Ag-NPs at 100 $\mu\text{g}/\text{mL}$, m6 with TiO₂-NPs at 50 $\mu\text{g}/\text{mL}$ and Ag-NPs at 25 $\mu\text{g}/\text{mL}$, m7 with TiO₂-NPs at 75 $\mu\text{g}/\text{mL}$ and Ag-NPs at 25 $\mu\text{g}/\text{mL}$.

The same experiments were repeated using 5 μL of the added NPs rather than 3 μL , and similar results were obtained. As shown in Figure 4, for the detection of all four *Aspergillus* species (*A. flavus*, *A. parasiticus*, *A. ochraceus*, and *A. fumigatus*), the amplification curve of mixture m (no NPs) appeared first, followed by those of m1 and m2, indicating partial inhibition. However, mixtures m3–m7 all showed complete inhibition of RTi-PCR. The amplification curves for *tub1*, *aflR*, *aflD*, and *aflM* (Figure 5). Figure 5a showed that the amplification curves for *tub1* two reactions m1 and m2 for pure Ag-NPs and the combination of Ag-NPs and TiO₂-NPs (2:1) exhibited partial RTi-PCR inhibition, whereas complete RTi-PCR inhibition was observed for the mixtures m3–m7. Figure 5b, c and d showed amplification curves for *aflR*, *aflD* and *aflM* genes with the same results for *tub1* gene.

We here demonstrate the inhibitory effects of Ag-NPs and TiO₂-NPs in real-time PCR detection. Ag-NPs and TiO₂-NPs were added to the real-time PCR system at two amounts (3 μL , 5 μL) and at various concentrations, either alone or in combination at different ratios for the detection of *Aspergillus* species and aflatoxin genes of *Aspergillus flavus*. We found that Ag-NPs resulted in partial inhibition of the reaction alone or at higher ratios in combination with TiO₂-NPs. However, TiO₂-NPs alone or at higher ratios in combination with Ag-NPs completely

inhibited the reactions. The majority of combinations at the higher amount (5 μL) also resulted in complete inhibition. However, the results of this study indicate that inclusion of Ag-NPs and TiO_2 -NPs in real-time PCR should be undertaken with caution, and only after thorough evaluation and validation of the impact of the Au-NPs on the assay under the specific conditions chosen for analysis.

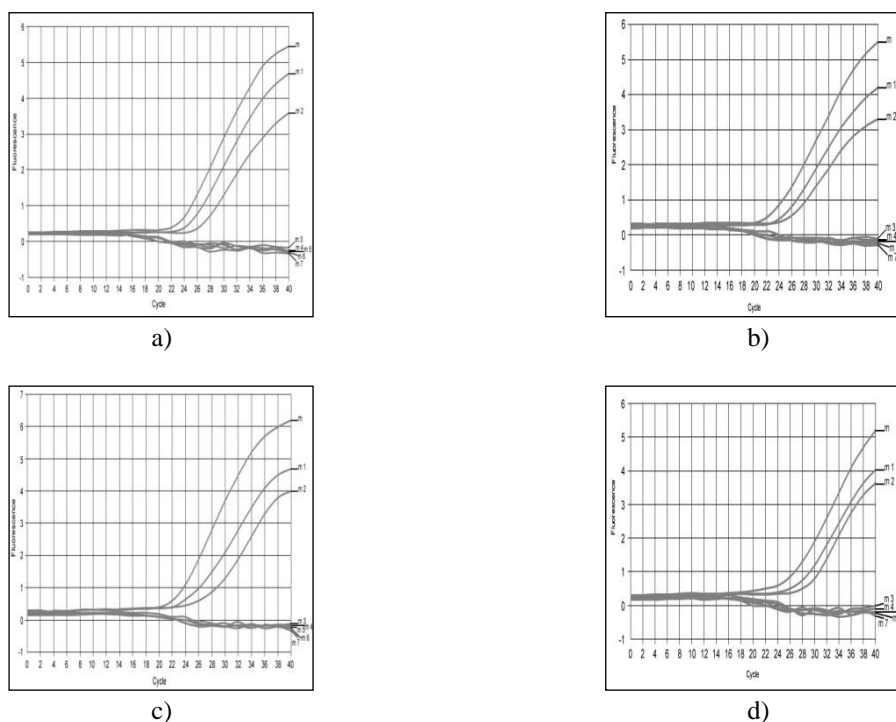


Fig. 4. Amplification curves of RTi-PCR for detection of a) *A. flavus*, b) *A. parasiticus* c) *A. ochraceus* d) *A. fumigatus* with 3 μL of different combinations of Ag-NPs and TiO_2 -NPs. (m) reference curve with no NPs, m1 with Ag-NPs at 100 $\mu\text{g}/\text{mL}$, m2 with Ag-NPs at 50 $\mu\text{g}/\text{mL}$ and TiO_2 -NPs at 25 $\mu\text{g}/\text{mL}$, m3 with Ag-NPs at 75 $\mu\text{g}/\text{mL}$ and TiO_2 -NPs at 25 $\mu\text{g}/\text{mL}$, m4, with Ag-NPs at 50 $\mu\text{g}/\text{mL}$ and TiO_2 -NPs at 50 $\mu\text{g}/\text{mL}$, m5 with TiO_2 -NPs at 100 $\mu\text{g}/\text{mL}$, m6 with TiO_2 -NPs at 50 $\mu\text{g}/\text{mL}$ and Ag-NPs at 25 $\mu\text{g}/\text{mL}$, m7 with TiO_2 -NPs at 75 $\mu\text{g}/\text{mL}$ and Ag-NPs at 25 $\mu\text{g}/\text{mL}$.

Several studies have shown that the combination of certain NPs can greatly improve the amount and stability of PCR products, which has led to an explosion in research on nanomaterials-based PCR for biological and biomedical applications [21] and [12] showed that the addition of TiO_2 -NPs significantly enhanced the PCR efficiency for various types of DNA templates, with an increase in the amount of PCR products and reduction in the reaction time when using the optimal concentration of TiO_2 -NPs. This performance improvement was largely attributed to the fact that TiO_2 -NPs show faster heat transfer and efficient denaturation cycles. It is possible that NPs increase the speed of the denaturation process at the NP surface initially (perhaps by some catalytic mechanism), which contributes to the time efficiency. However, [13] showed that Ag-NPs and/or TiO_2 -NPs could cause partial or complete inhibition of real time PCR, with the latter showing a stronger inhibitory effect. Thus, the complex interaction mechanism between Ag-NPs and TiO_2 -NPs remains somewhat of a mystery, which warrants further exploration with more solid experiments.

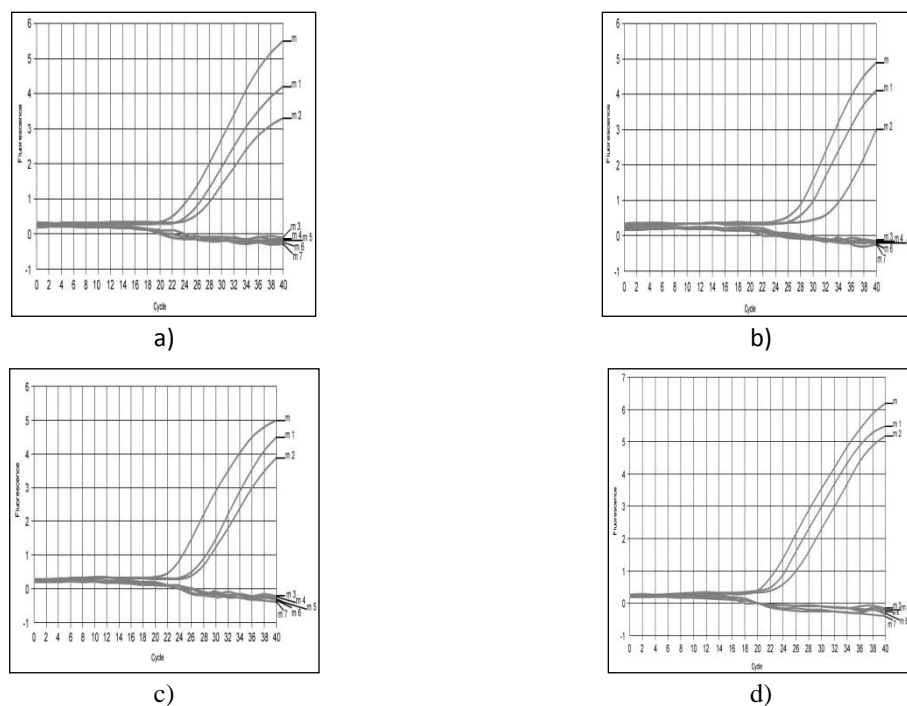


Fig. 5. Amplification curves of the four genes, a) *tub1*, b) *aflR*, c) *aflD* and d) *aflM* with 5 μL of different combinations of Ag-NPs and TiO_2 -NPs. (m) reference curve with no NPs, m1 with Ag-NPs at 100 $\mu\text{g}/\text{mL}$, m2 with Ag-NPs at 50 $\mu\text{g}/\text{mL}$ and TiO_2 -NPs at 25 $\mu\text{g}/\text{mL}$, m3 with Ag-NPs at 75 $\mu\text{g}/\text{mL}$ and TiO_2 -NPs at 25 $\mu\text{g}/\text{mL}$, m4, with Ag-NPs at 50 $\mu\text{g}/\text{mL}$ and TiO_2 -NPs at 50 $\mu\text{g}/\text{mL}$, m5 with Ag-NPs at 100 $\mu\text{g}/\text{mL}$, m6 with TiO_2 -NPs at 50 $\mu\text{g}/\text{mL}$ and Ag-NPs at 25 $\mu\text{g}/\text{mL}$, m7 with TiO_2 -NPs at 75 $\mu\text{g}/\text{mL}$ and Ag-NPs at 25 $\mu\text{g}/\text{mL}$.

Evaluation of ZnO-NPs (35 nm) and TiO_2 -NPs (100 nm) on the PCR-based detection of the *lacZ* gene of *Escherichia coli* and the 16S rRNA gene of *Pseudomonas aeruginosa*. They found that ZnO-NPs (0.4 mg/mL) highly enhanced the amount and purity of the PCR products for both genes, with an approximate 50% reduction in the total reaction time achieved by using the two types of NPs [23].

Evaluated the effects of the addition of Au-NPs with diameters ranging from 5 nm to 20 nm on RTi-PCR. Low concentrations of Au-NPs did not show any obvious effect on the reaction, whereas reaction inhibition became more apparent as the NP concentration increased. It was shown that the interaction and binding of Au-NPs to *Taq* polymerase reduced the concentration of free polymerase and therefore contributed to the inhibition of the RTi-PCR [24,25].

Nevertheless, adding an optimal concentration of Au-NPs into the PCR reagent mixture for RTi-PCR increased the PCR efficiency and shortened the reaction time, yielding greater amounts of PCR products and increasing the heating/cooling rates. In particular, the addition of Au-NPs increased the sensitivity of PCR detection by at least 7-fold and 4-fold compared to conventional PCR and RTi-PCR, respectively. The intrinsic thermal properties of NPs allows the thermal conductivity to be increased by >20% when the NPs are suspended in water, so that the heat flux is transported resulting in thermal equilibrium with the environment. These properties of Au-NPs are very important factors for the performance of PCR machines [26].

4. Conclusions

We believe that our study makes a significant contribution to the literature because NPs have been considered to improve the performance and efficiency of conventional and real-time PCR owing to their intrinsic thermal properties; however, inhibition has also been detected, and

the results are inconsistent. Our study stresses the importance of considering the optimal concentration, type, and combination of NPs to be included in real-time PCR. In addition, most of the work conducted to date on NPs in PCR has focused on gold NPs; therefore, our study contributes to the general literature on the application of nanomaterials in biotechnology.

Acknowledgement

The authors would like to extend their sincere appreciation to the Deanship of the Scientific Research at King Saud University for funding of this research through the Research Group Project no. RGP-269.

References

- [1] G. K. Stylios, P. V. Giannoudis, T. Wan. *Injury***36**, 1 (2005)
- [2] M. C. Reddy, K. S. R. Murthy, A. Srilakshmi, *African journal Biotechnology***14**, 222 (2015).
- [3] R. K. Saiki, D. H. Gelfand, S. Stoffel, *Science***239**, 487(1988).
- [4] Y.Ch. Swaran, *Malaysian Journal of Forensic Sciences* **5**, 12 (2014).
- [5] H. An and B. Jin, *Biotechnology Advances* **30**, 1721 (2012).
- [6] J. S. De Bono, S. Oudard, M.Ozguroglu, *Lancet***376**,1147 (2010).
- [7] C. Kneuer, M. Sameti, E. G.Haltner, *International Journal of Pharmaceutics* **196**, 257(2000).
- [8] A. L. Haber, K. R. Griffiths, A K Jamting, *Analytical and Bioanalytical Chemistry* **392**,887(2008).
- [9] S. Basu, .S Jana, S. Pande, *J. Colloid Interface Science* **321**, 288 (2008).
- [10] A. G. Pershina, A. E. Sazonov, V.D. Filimonov, *Russian Chemical Reviews* **83**, 299(2014).
- [11] S. Bansod, S. Bonde, V. Tiwari, *Journal of Biomedical Nanotechnology* **9**, 1962(2013).
- [12] R. Abdul Khaliq, P. J. Sonawane, B. K. Sasi, *Nanotechnology* **2010**, 1 (2010).
- [13] W Wan and T Yeow, *9th IEEE Conference on Nanotechnology*, 458(2009).
- [14] AR Abd El-Aziz, MR Al-Othman, SA Eifan, *Digest Journal of Nanomaterials and Biostructures* **8**, 1215 (2013).
- [15] S. Ganapathy and K. Siva, *International Journal of Advanced Life Sciences* **4**, 69 (2016).
- [16] M. A, Mahmoud.2015. *Foodborne Pathogen Disease* **12**, 289 (2016).
- [17] Y. Luo, W. Gao, M. Doster., *Journal of Applied Microbiology* **106**, 1649 (2009).
- [18] R. Bu, R. Sathiapalan, M. Ibrahim, *Journal of Medical Microbiology* **54**, 243 (2005).
- [19] N. Sardiñas, C. Vázquez, J. Gil-Serna, *International Journal of Food Microbiology* **145**, 121(2011).
- [20] H. Schmidt., M. Bannier, R.Vogel, *Letters in Applied Microbiology* **38**, 464 (2004).
- [21] A Bintvihok, S Treebonmuang, K Srisakwattana, Nuanchun W, Patthanachai K, *Toxicology Research* **32**, 81 (2016).
- [22] Dun P, Yangqin W, Lijuan M, Chunhai F, Jun H, (2011).
- [23] AM Fadhil, MR Al-Jeboory, MH Al-Jailawi, *International Journal of Current Microbiology and Applied Sciences* **3**, 549 (2014).
- [24] Wan W, Yeow JT, Van Dyke MI. *Conference Proc. IEEE Eng. Med. Biol. Soc.* 2771 (2009).
- [25] BV Vu, D, Litvinov, RC Willson, *Analytical Chemistry* **80**, 5462 (2008).
- [26] Li M, Yu-Cheng L, W Chao-Chin, L Hsiao-Sheng, *Nucleic Acids Research***33**, e184 (2005).